Strategies to Improve the Barrier and Mechanical Properties of Pectin Films for Food Packaging: Comparing Nanocomposites with Bilayers

Victor Gomes Lauriano Souza [1,2,]*, Igor Penido Mello [1,3], Omer Khalid [1,3], João Ricardo Afonso Pires [1], Carolina Rodrigues [1], Marta M. Alves [4], Catarina Santos [4,5], Ana Luísa Fernando [1] and Isabel Coelhoso [3,]*

1   MEtRICs, Departamento de Ciências e Tecnologia da Biomassa, NOVA School of Science and Technology, FCT NOVA, Campus Caparica, Universidade NOVA de Lisboa, 2829-516 Caparica, Portugal; igorpenidodemello@gmail.com (I.P.M.); omerkhalid2626@yahoo.com (O.K.); jr.pires@campus.fct.unl.pt (J.R.A.P.); cpe.rodrigues@campus.fct.unl.pt (C.R.); ala@fct.unl.pt (A.L.F.)
2   International Iberian Nanotechnology Laboratory (INL), Av. Mestre José Veiga s/n, 4715-330 Braga, Portugal
3   LAQV-REQUIMTE, Departamento de Química, NOVA School of Science and Technology, FCT NOVA, Campus Caparica, Universidade NOVA de Lisboa, 2829-516 Caparica, Portugal
4   CQE Instituto Superior Técnico, Universidade de Lisboa, Av. Rovisco Pais, 1049-001 Lisboa, Portugal; martamalves@tecnico.ulisboa.pt (M.M.A.); catarinafsantos@tecnico.ulisboa.pt (C.S.)
5   EST Setúbal, CDP2T, Campus IPS, Instituto Politécnico de Setúbal, 2910-761 Setúbal, Portugal
*   Correspondence: victor.souza@inl.int (V.G.L.S.); imrc@fct.unl.pt (I.C.)

Abstract: Traditional food packaging systems help reduce food wastage, but they also produce environmental impacts when not properly disposed of. Bio-based polymers are a promising solution to overcome these impacts, but they have poor barrier and mechanical properties. This work evaluates two strategies to improve these properties in pectin films: the incorporation of cellulose nanocrystals (CNC) or sodium montmorillonite (MMT) nanoparticles, and an additional layer of chitosan (i.e., a bilayer film). The bionanocomposites and bilayer films were characterized in terms of optical, morphological, hygroscopic, mechanical and barrier properties. The inclusion of the nanofillers in the polymer reduced the water vapor permeability and the hydrophilicity of the films without compromising their visual properties (i.e., their transparency). However, the nanoparticles did not substantially improve the mechanical properties of the bionanocomposites. Regarding the bilayer films, FTIR and contact angle studies revealed no surface and/or chemical modifications, confirming only physical coating/lamination between the two polymers. These bilayer films exhibited a dense homogenous structure, with intermediate optical and hygroscopic properties. An additional layer of chitosan did not improve the mechanical, water vapor and oxygen barrier properties of the pectin films. However, this additional layer made the material more hydrophobic, which may play an important role in the application of pectin as a food packaging material.

Keywords: bilayers; bionanocomposites; montmorillonite; cellulose nanocrystals; pectin; chitosan

1. Introduction

Around 1.7 billion tonnes of food—one-third of all food produced globally—is lost or wasted along the food chain [1]. Food loss, an issue at the production, distribution and storage phases, is more significant in developing countries, while food waste, caused at retail and consumer levels, is more serious in developed countries [2]. Both problems, together called food wastage, not only represent economic losses but also cause unnecessary environmental impacts such as greenhouse gases emissions, water usage and land occupation and ultimately constitute another barrier to overcoming world hunger [1].

Appropriate packaging can reduce food wastage at almost every stage of the food chain. Packaging systems are responsible for protection during transportation and the storage of food products but should also have other characteristics to fight food wastage.

They must be easy to open, easy to empty, be resealable, contain portions of appropriate size and provide gas and water vapor barrier properties to the content [3].

Many plastic materials offer the desirable characteristics for packages, most of which are from petrochemical sources. However, 30% of plastics used for packaging are not eligible for recycling. This may be due to incompatible polymers, the small size of plastic parts, multilayered materials or the difficulty of cleaning the organic material [4]. While increasing the amount and number of materials involved in the packaging helps products last longer on shelves and in households, it also creates more environmental impacts. This trade-off between the packaging footprint and food wastage can only be evaluated through life cycle assessment studies [5].

At best, packaging design should aim simultaneously at decreasing food wastage and the environmental impact of the package itself [6]. In this sense, biodegradable polymers represent a major trend in materials that minimize impacts on landfills compared to fossil-based ones [7]. Bio-based films made of polysaccharides (e.g., chitosan, pectin, cellulose and pullulan) have been studied for this purpose and are a natural alternative aligned with circular economy principles. They are biodegradable and can be derived from plant resources, food industry and agriculture by-products, all of which contribute to reduce waste in a circular-economy approach [8,9]. These materials offer an appropriate barrier to oxygen, biocompatibility and are eco-friendly [10]. These properties make them candidates for their utilization as films and coatings in the food packaging industry [6]. Moreover, the incorporation of ingredients rich in bioactive compounds (e.g., essential oils, propolis and protein hydrolysates) into these films and coatings may enhance packaging activity (i.e., antimicrobial, antioxidant activities), thus delaying food degradation [6,9,11,12]. Out of these materials, chitosan and pectin have excellent film-forming characteristics [13].

Pectin, a structural non-toxic anionic polysaccharide contained in the cell walls of many fruits, is used in the food industry as a thickening and stabilizing agent [14]. The monomer is galacturonic acid containing methylated ester groups [15,16]. The extent of methylated groups (DE) classifies it as either low methoxyl pectin (DE < 50) and high methoxyl pectin (DE > 50) [17]. As mentioned, pectin has been studied to produce bio-based films. The major mechanism of film formation involves the breaking of polymer segments and the reforming of the polymeric chains by evaporating the solvent, thus creating hydrophilic and hydrogen bonds [18]. Nonetheless, pectin films face the same challenge associated with bio-based polymers, especially polysaccharides, which is the lack of good mechanical properties [19]. Furthermore, although they present a good barrier to oxygen, their hydrophilic characteristics makes them permeable to water vapor, which limits their application [20].

One strategy to achieve a better performance in these renewable materials is the addition of nanomaterials to produce bionanocomposites [21,22]. Nanoparticles (NPs) interact physically and chemically with polymeric chains to create stronger and reinforced structures that present improved barrier and mechanical properties. Inorganic nanoparticles, such as montmorillonite (MMT), and organic NPs, carbon nanotubes or nanocellulose have been used in many studies as reinforcements to improve the mechanical characteristics of different biofilms [23]. Among nanoclays, montmorillonite (MMT) is of particular interest. It consists of stacked silicate sheets with a high aspect ratio (ratio of length to thickness). It can enhance the mechanical properties of polymeric materials when the nanoclay sheets are well dispersed and exfoliated in the matrix [18,24]. Cellulose nanocrystals (CNC) are another filler employed in composites. These biopolymeric assemblies have gained attention due to their unique morphology, low cost and availability [25]. Again, good dispersibility is paramount for achieving significant mechanical improvements [26].

An alternative strategy used to improve the barrier and mechanical properties of bio-based polymers is through the combination of two or more biopolymers in blends or layers [21,27]. The development of multilayered biopolymer films is a recent trend in the food packing industry, such as the combination of chitosan with different anionic polymers [28,29], including pectin. Indeed, there are several studies available in the

literature which show that there is a huge crosslinking potential between chitosan and pectin. This is due to the strong electrostatic interactions (Figure 1) between the protonated amino groups of chitosan and the carboxylate side chains of pectin [30]. This cross-linking imparts barrier and mechanical properties that make this bilayer combination favorable for food applications.
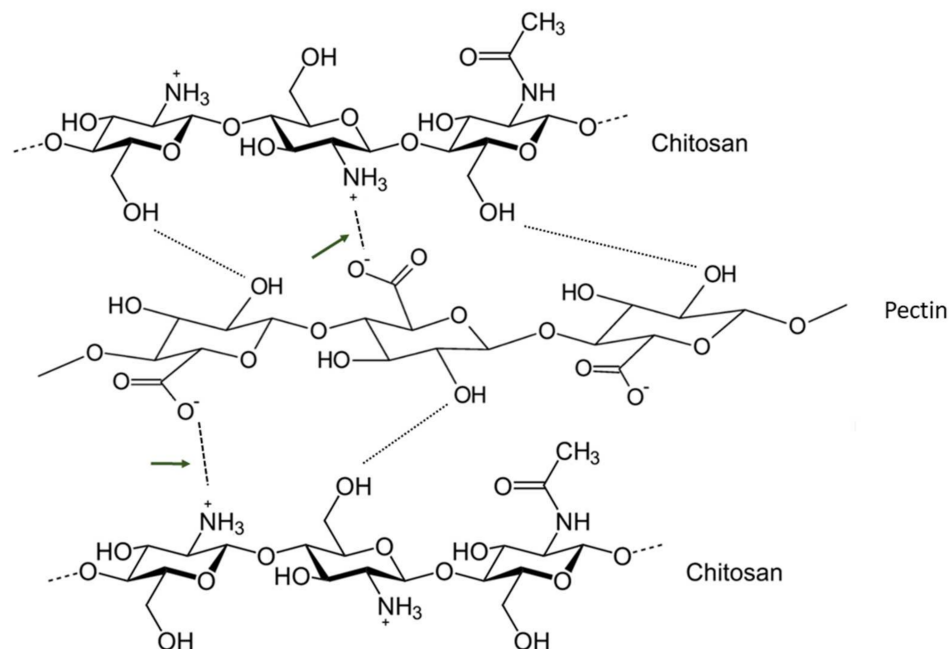

Figure 1. Electrostatic interaction between chitosan and pectin.

Yet, to the best of our knowledge, there are no studies reported in the literature that compares the use of nanocomposites with the use of bilayers as strategies to improve the barrier and mechanical properties of pectin films for food packaging. Thus, this work aimed to compare these different strategies to improve pectin properties by designing both bionanocomposites incorporated with inorganic (MMT) or organic (CNC) NPs and bilayer films, made by adding a polymeric layer of chitosan to pectin. The mechanical, barrier and optical alterations achieved with these strategies were compared with pristine pectin and discussed. Finally, the study intends to add knowledge regarding the applicability of biopolymers for food packaging and whether they are a suitable alternative for traditional non-biodegradable packaging films currently in use.

2. Materials and Methods

2.1. Materials and Reagents

Commercial pectin from citrus peel (Poly-D-galacturonic acid > 74.0 %) and chitosan (Poly(D-glucosamine)) with 75% of deacetylation and high molecular weight (31–37 kDa) were obtained from Sigma-Aldrich (Steinheim, Germany). MMT (Cloisite-Na$^+$) was kindly supplied by BYK Additives (Wesel, Germany) and CNC (5%–15%) by Nanocrystacell (Podcerkev, Slovenia). Glycerol and glacial acetic acid were purchased from Alfa Aesar (Kandel, Germany), while sodium chloride and potassium acetate from Sigma-Aldrich (Dorset, UK). All water was purified using the Milli-Q system from Millipore (Billerica, MA, USA).

2.2. Production of Films

Five different formulations were tested in this experiment, namely: pristine pectin film, pectin + MMT, pectin + CNC, pristine chitosan film (chitosan) and bilayer pectin/chitosan. The films were produced using the casting method as described below.

2.2.1. Production of Pectin Film and the Bionanocomposites

The pectin films were produced according to Oliveira et al. (2016) [22] and Souza et al. (2019) [24]. To produce the filmogenic dispersion (FD), 2.3 wt.% pectin was dissolved in water with 27 wt.% glycerol (in terms of dry pectin). The dispersion was homogenized with a T18 Ultra-Turrax disperser (IKA®T18, Staufen, Germany) at 11,000 rpm for 45 min. MMT and CNC were weighed and added individually to the pectin solution (2.5 wt.% of each, in dry pectin). The nanoparticles were dispersed with three cycles of 5 min under agitation (15,000 rpm) followed by 15 min in ultrasound batch (Selecta, Barcelona, Spain). Each film type (pure pectin, pectin + MMT and pectin + CNC) was cast using 140 mL of dispersion on glass plates (18 cm × 25 cm) and left to dry at 30 °C for 72 h. The dry films were later detached from the plates and kept in aluminum foils at room temperature for the analysis.

2.2.2. Production of Pristine Chitosan Film

Pristine chitosan films were produced according to [24]. To produce the FD, 1.5 wt.% chitosan was dissolved in 1% *v/v* of acetic acid solution overnight. As a plasticizer, 30 wt.% glycerol (in terms of dry chitosan) was added to the FD. Then the dispersion was homogenized with a high-speed disperser (T18 Ultra-Turrax) at 15,000 rpm for 5 min, followed by 15 min in ultrasound batch to remove the air bubbles. Then, the CH films were cast using 140 mL of dispersion on glass plates (18 cm × 25 cm) and left to dry at 30 °C for 72 h. The dry films were later detached from the plates and kept in aluminum foils at room temperature for the analysis.

2.2.3. Production of Bilayer Pectin/Chitosan

The same protocol was used to synthesize both pristine chitosan and pectin dispersion for the preparation of bilayer films. For the first layer, 100 mL of the chitosan dispersion was cast on a glass mold and left to dry at 30 °C for approximately 24 h. Before the film was completely dried, 100 mL of the pectin dispersion was poured onto this semi-dried chitosan film and left to dry at 30 °C for 72 h. The dry films were later detached from the plates and kept in aluminum foils at room temperature.

2.3. Characterization of Films

2.3.1. Scanning Electron Microscopy

The morphology of the film surface was analyzed by scanning electron microscopy (SEM) using a JEOL JSM-7001F (Tokyo, Japan) piece of equipment with an energy beam of 15 kV and a working distance of 10 mm. The elemental chemical composition was evaluated using a coupled X-ray energy dispersive spectrometer (EDS) (JEOL, Tokyo, Japan). The films' conductivity was increased by applying a thin layer of gold/palladium with a Polaron E-5100 (Quorum Technology, Hertfordshire, UK).

2.3.2. X-ray Diffraction

The crystal structure of the films was analyzed using X-ray diffraction (XRD; Bruker D8 ADVANCE Powder Diffractometer) with monochromatic CuKα (target) radiation (1.5405 Å) at a scan rate of 0.05°/s.

2.3.3. Water Vapor Permeability

The *WVP* was measured using the gravimetric method [31]. Two samples of each film type were put on the top of 45 mm diameter glass cells containing 8 mL of saturated NaCl solution (relative humidity (RH) of 76.9%), and they were then sealed and placed inside a desiccator with saturated potassium acetate solution (RH = 22.5%). A fan promoted circulation inside the desiccator to avoid the formation of a stagnant layer above the films.

The temperature was kept at 30 °C. Water vapor flux through the films was assessed by weighing the cells at regular time intervals for 5 h. The *WVP* was given by Equation (1):

$$WVP = N_W \times \delta / \Delta P_w \tag{1}$$

where N_W (mol/m^2·s) is the water vapor flux, δ (m) is the film thickness and ΔP_w, (Pa) is the effective driving force ($p_{w2} - p_{w1}$). With the relative humidity in and outside the cell, water vapor pressure ($P*$) and considering the diffusion through a stagnant film model, Equations (2–4) can be applied:

$$p_{w1} = RH_{in} \times P* \tag{2}$$

$$p_{w3} = RH_{out} \times P* \tag{3}$$

$$N_W = (P/RTZ) \times D_{w-air} \times \ln(P - p_{w2}/P - p_{w1}) \tag{4}$$

where $P*$ is the atmospheric pressure (Pa), R the universal gas constant (J/mol·K), T the absolute temperature (K), z the average height (m) of the gap between the NaCl solution and the film and D_{w-air} the diffusion coefficient of water vapor in the air (m^2/s).

2.3.4. Oxygen Permeability

Oxygen permeability (OP) was measured according to the method described in [31]. Each film was put between two identical stainless steel chambers that remained at 30 °C through the use of a thermostatic bath. One of the chambers was loaded with pure oxygen at 0.7 bar and pressure transducers measured the pressure change over time on both sides. The permeability was given by the following expression (Equation (5)):

$$(1/\beta) \times \ln(\Delta p_0 / \Delta p) = P \times (t/\delta) \tag{5}$$

where $P*$ is the geometric parameter of the cell, Δp the pressure difference between the two compartments, P (mol·m/m^2·s·Pa) the oxygen permeability, t (s) the time and δ (m) the film thickness. The cell was calibrated using a PDMS film with known permeability.

2.3.5. Optical Properties

Surface color, opacity and transparency were evaluated. The color was measured according to the L*a*b* color space for five samples using a CR-410 colorimeter (Konica, Japan). In this system, L* measures perceptual lightness, $a*$ the red–green axis and $b*$ the blue–yellow axis. The chroma C* (Equation (6)) and the hue angle h° (Equation (7)) are the polar coordinates considering a cylindrical model [24].

$$C* = (a^2 + b^2)^{0.5} \tag{6}$$

$$h° = atan\ (b*/a*) \tag{7}$$

The opacity was assessed by reading the absorbance at 600 nm of three samples using a UV/VIS spectrophotometer (Spekol 1500, Analytikjena, Germany) through Equation (8) [24].

$$Opacity = A_{600nm}/\delta \tag{8}$$

where δ is the film thickness (mm). The film transparency was determined by a spectrum scan from 200 to 900 nm with the same equipment, expressed as transmittance (%).

2.3.6. Contact Angle

The contact angle (θc) is an indicator of the wettability of a surface. Here, the sessile drop technique was used to measure the contact angle of a droplet of water on the films (Clegg, 2013). The measurements were done using a goniometer (KSV Instruments, CAM-100, Helsinki, Finland) with the software CAM 100, in which the angle was given as an average on both sides of the drop [24].

2.3.7. Humidity, Swelling and Solubility in Water

Humidity tests were carried out by oven drying at 105 °C for 24 h and expressed as g of water/g of humid material, with samples being weighed on an analytical scale (Mettler Toledo AB204, Switzerland) with a precision of 0.0001 g [24].

Rectangular specimens of 2 cm × 2 cm dimensions were briefly collected and weighed on an analytical balance (M1). These samples were then conditioned in a natural convection oven (WTB binder, Germany) at 70 °C for 24 h and then re-weighed (M2).

For the determination of swelling and solubility in water, the dried films with mass were placed in a Petri dish containing 30 mL of Milli-Q water and stored for 24 h at room temperature. Water from these dishes was removed after 24 h, and the samples were gently dried using tissue paper and weighed on an analytical scale (M3). These films were then re-dried in a natural convection oven at 70 °C for 24 h before being re-weighed (M4).

Humidity, degree of swelling and solubility in water (g/100 g of films) were calculated according to Equations (9)–(11).

$$\%Humidity = ((M1 - M2)/(M1)) \times 100 \tag{9}$$

$$\%Swelling\ degree = ((M3 - M2)/(M2)) \times 100 \tag{10}$$

$$\%Solubility = ((M4 - M2)/(M2)) \times 100 \tag{11}$$

where *M1* is the initial mass of the films, *M2* is the dried mass of the film, *M3* is the mass of the films after absorbing water (after 24 h in contact with water) and *M4* is the dried mass of the films after being in contact of water for 24 h.

2.3.8. Thickness and Mechanical Properties

The thickness of the films was measured with a micrometer (0.001 mm, Mitutoyo, Kawasaki, Japan) at five different points. The modulus of elasticity (E), tensile strength (TS) and elongation at break (EAB) were measured according to ASTM D882-12 [32]. Strips of the films (150 mm × 25 mm) were mounted in the tensile grips of the load cell (Autograph Shimadzu, Sydney, Australia), with an initial gauge length of 50 mm and stretched at 50 mm/min until the breakage.

2.3.9. ATR-FTIR Spectroscopy

Attenuated total reflectance Fourier transform infrared spectroscopy (ATR-FTIR) spectra of the films were obtained using a FTIR spectrometer (PerkinElmer Spectrum Two, Perkin Elmer, Waltham, MA, USA) from 4000 to 650 cm^{-1} with 1 cm^{-1} resolution and 32 scans [33].

2.3.10. Experimental Design and Statistical Analysis

The experiments were conducted using a completely randomized design with three replications.

Statistical analysis of data was performed through a one-way analysis of variance (ANOVA) and, when applicable, the differences among mean values were processed using the Tukey test. In both cases the Software OriginLab, version 8.5 (OriginLab Corporation, Northampton, MA, USA) was used. Pristine chitosan film was not included in the statistical analysis once it had been prepared to be used as a reference in the analysis of the bilayer films.

All requirements necessary to carry out the ANOVA (namely, normality of data and homogeneity of variances) were validated. Significance was defined at $p < 0.05$ and the results were expressed as the means of the replications ± standard deviation.

3. Results and Discussion

The bionanocomposites and bilayer films were successfully produced using the casting method. After being dried and detached, they had a transparent and mostly homogeneous aspect, with an apparent yellowish color (Figure 2).

Figure 2. Pectin film produced.

3.1. Characterization of Films

3.1.1. SEM and X-Ray Diffraction

The physicochemical results presented in Figure 3 show that it is possible to incorporate different NPs in the pectin films. Figure 3 shows the used CNC (Figure 3a) and MMT (Figure 3b) NPs and demonstrates that the CNC NPs have a fiber morphology with an average length of 200 nm and a thickness of 20 nm, whereas the MMT NPs have a platelet like morphology with an average diameter size of ~30 nm. The SEM images prove that both particles are nanometric at least in one of the dimensions. Chemical element composition analysis of these particles showed the presence of carbon and oxygen (data not shown) on the organic CNC NPs, whereas the presence of Na, Al and Si, as well as that of O, was detected on the inorganic MMT NPs (Figure 3b). The XRD patterns of the CNC and MMT NPs (Figure 3i,j, respectively) agree with those reported in the literature [34,35].

Figure 3 shows the SEM images of a pectin film (Figure 3d) loaded with CNC (Figure 3c) or loaded with MMT (Figure 3e) NPs. It is observed that the surface morphology of the pectin films did not suffer significant modification through the addition of the NPs (Figure 3c–e). Although the amount of incorporated NPs in the films was reduced, it was still possible to detect them on the surface of the bionanocomposite films, as seen in the magnified figure insets in Figure 3c,e.

The thickness of pectin (Figure 3g), pectin + CNC (Figure 3f) and pectin + MMT (Figure 3h) films, determined by SEM imaging, revealed that this is close to 40 μm for all the newly developed films. This observation confirms that the presence of the NPs has not affected the thickness of the bionanocomposites when compared with pectin alone.

While the chemical elemental analysis of the organic particles in pectin was inconclusive, as both are carbon-based compounds, that of the inorganic particles was thoroughly accessed by detecting Na, Al and Si (Figure 3k), coincident with the corresponding morphological features (inset in Figure 3e). A detailed analysis was made by X-ray (Figure 3i,j). The diffractogram of pectin agrees with the as-cast films reported in the literature [36]. When analyzing the diffractograms of the bionanocomposites, the presence of CNC NPs in the pectin + CNC film (Figure 3i) was confirmed by the presence of two additional bands detected in the XRD spectrum between 10–20 2theta (Θ); the presence of MMT NPs in the pectin + MMT film was inconclusive by XRD, most probably due to the low detection limit of the technique (Figure 3j).
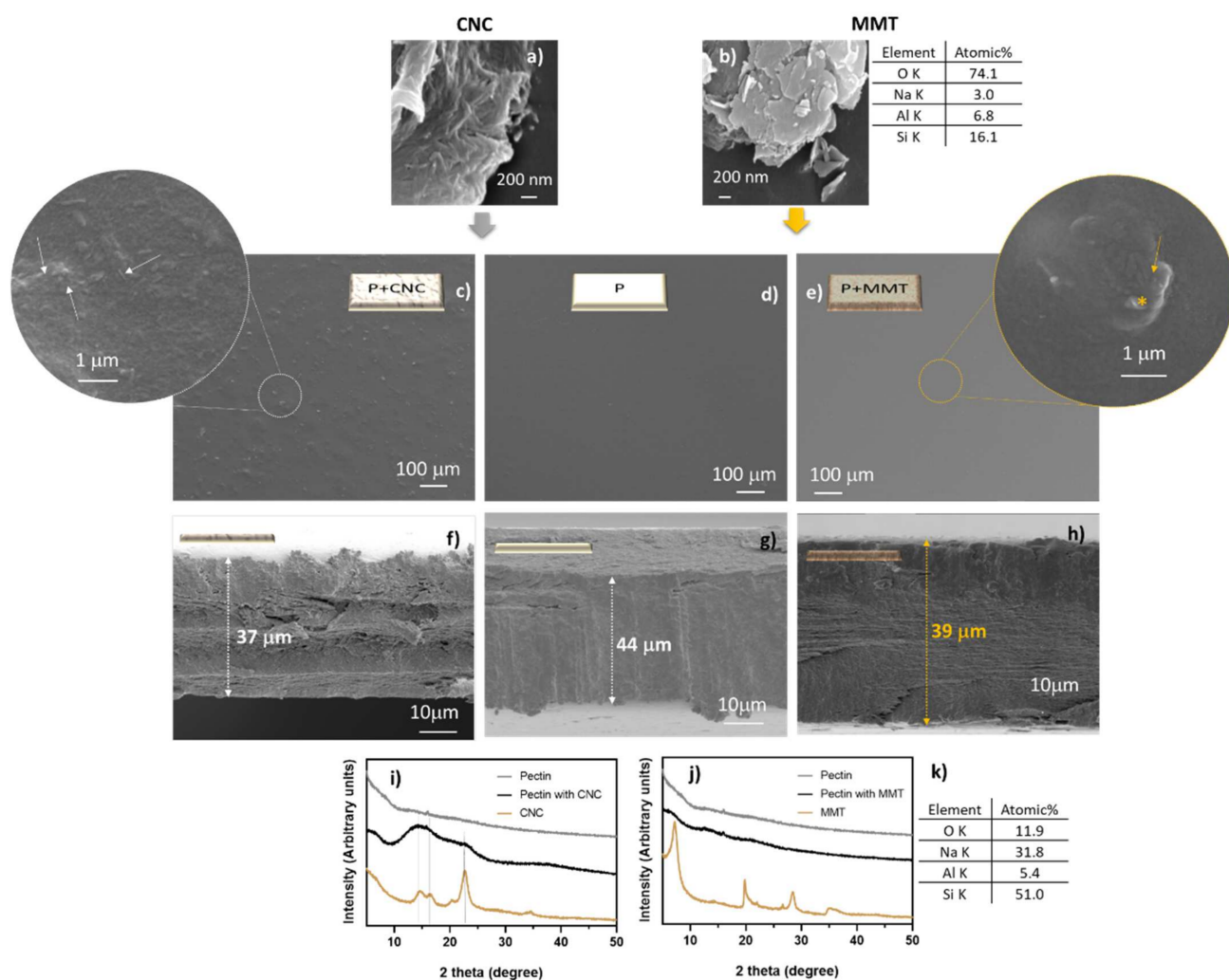
Figure 3. Physicochemical characterization of the bionanocomposites. Scanning electron microscopy (SEM) images of the CNC (**a**) and MMT (**b**) NPs with the corresponding chemical elemental composition presented for the MMT NPs; SEM top-view images of pectin films (**d**), pectin loaded with CNC (**c**), or loaded with MMT (**e**) and respective SEM cross-section images (**f-h**), with the corresponding thicknesses; X-ray diffraction (XRD) diffractograms (**i,j**) of the bionanocomposites and chemical elemental composition of the pectin film loaded with MMT determined by energy dispersive X-ray spectroscopy (EDX) (**k**). * Inset in magnified Figure 3e correspond to the NPs loaded in the bionanocomposites.

Due to the different nature of the NPs used in the formulation of the bionanocomposites, different chemical analyses were required to prove their incorporation in pectin, namely EDX for MMT NPs and XRD for CNC NPs (Figure 3).

However, the presence of chemical elements characteristic of MMT NPs was observed using EDX analysis, which confirms the presence of MMT in P + MMT films (Figure 3k). The disappearance of the characteristic MMT peak at $2\Theta = 7.20$ may indicate that the NPs achieved an exfoliated configuration within the polymer, once there was an enhancement of the basal spacing between the individual MMT layers (inter-lamellar distance or d_{001}), which enabled the interaction of the polymer chain and the MMT resulting in this amorphous structure [37,38]. Moreover, the improvement in the film's barrier and mechanical properties with the incorporation of MMT was achieved when the NP was in an exfoliated or intercalated configuration [39], which corroborates the results discussed in Sections 3.1.5, 3.1.6 and 3.1.8.

Figure 4 shows the physical characteristics of the bilayer films. It indicates that the chitosan film has a homogenous morphology (Figure 4a), a thickness of 47 μm (Figure 4b) and a diffractogram coincident with that reported in the literature by Billah et al. (2020) [40]. The bilayer film, designed by adding chitosan on the top of pectin, as in the bionanocomposite films (Figure 3), resulted in unaltered surface morphologies (Figures 3d and 4) either on the pectin or the chitosan surfaces. The bilayer film exhibits a thickness of around 59 μm (Figure 3d), corresponding to 34 μm of pectin thickness and 25 μm of chitosan thickness. A deeper inspection of the interface between the pectin and chitosan interface shows a perfect interaction with no signs of cracks or porous regions, suggesting that strong electrostatic and cross-linking interactions were attained on this bilayer film [30]. The analysis of the FTIR spectra in Section 3.1.2 will help to provide more information about these films and to corroborate this claim.
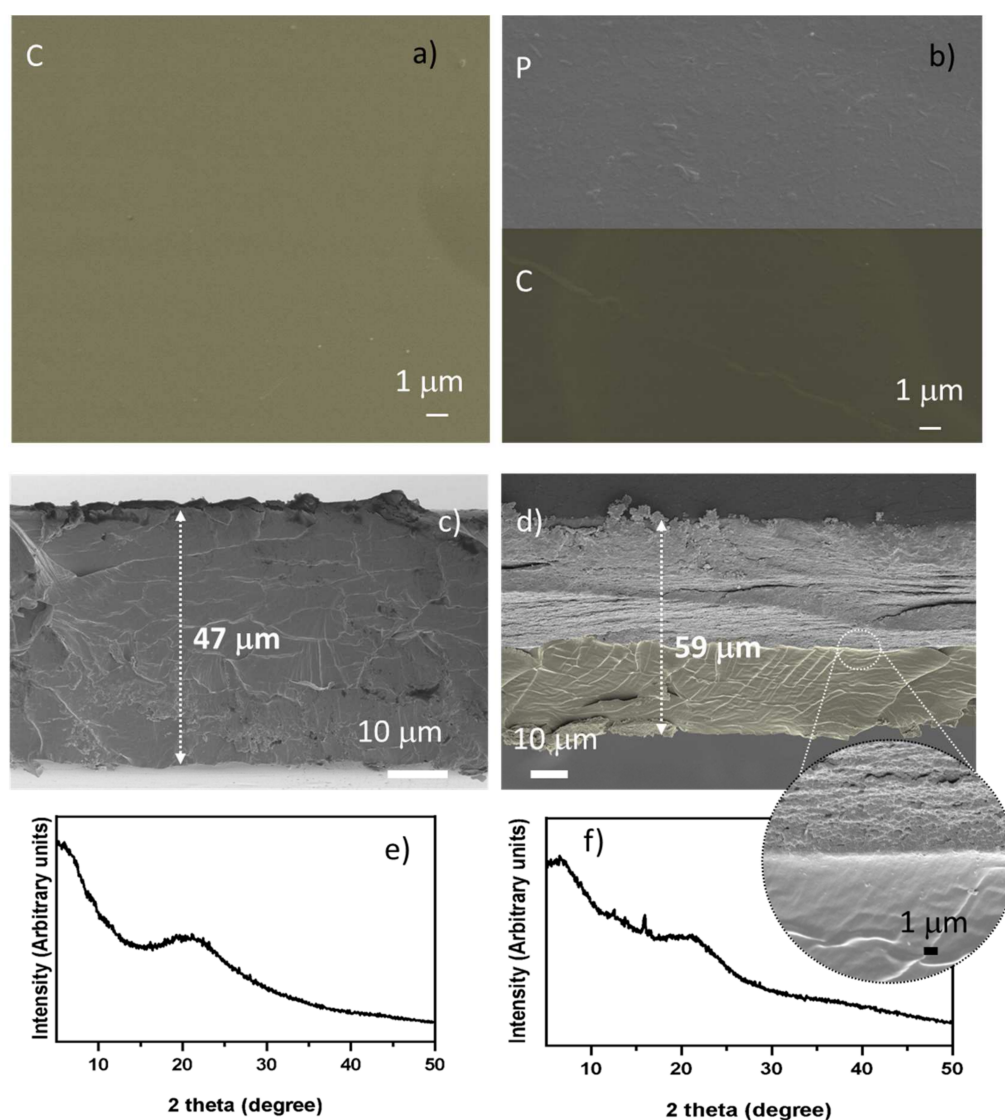
Figure 4. Physicochemical characterization of the bilayer films. Scanning electron microscopy (SEM) top-view images of chitosan (**a**), pectin and chitosan (**b**) films, and respective SEM cross-section images (**c**,**d**), with the corresponding thicknesses; X-ray diffraction (XRD) diffractograms (**e**,**f**) of the chitosan and bilayer films, respectively.

In the diffractogram of the bilayer film (Figure 4f), a clear contribution of both the pectin (Figure 3i) and chitosan (Figure 4e) reflection peaks can be depicted between 5–30 2theta (Θ), proving the successful design of a chitosan–pectin bilayer film.

3.1.2. FTIR Spectroscopy

Fourier transform infrared spectroscopy is a useful technique for the purpose of evaluating the chemical composition and bonds established between atoms in a material [41]. The characteristic peaks of pectin are depicted in Figure 5. The intensive bands at around 1697 and 1221 cm^{-1} observed for all pristine pectin film and bionanocomposites are related to the vibrations of the carbonyl in the methyl ester (COOCH$_3$) [42]. The band around 1606 cm^{-1} is due to the vibrations of the dissociated carboxyl group (COO$^-$). The nanoparticles did not produce differences in the FTIR spectra of the films (Figure 5), which can be explained by the small amount of fillers added [33].
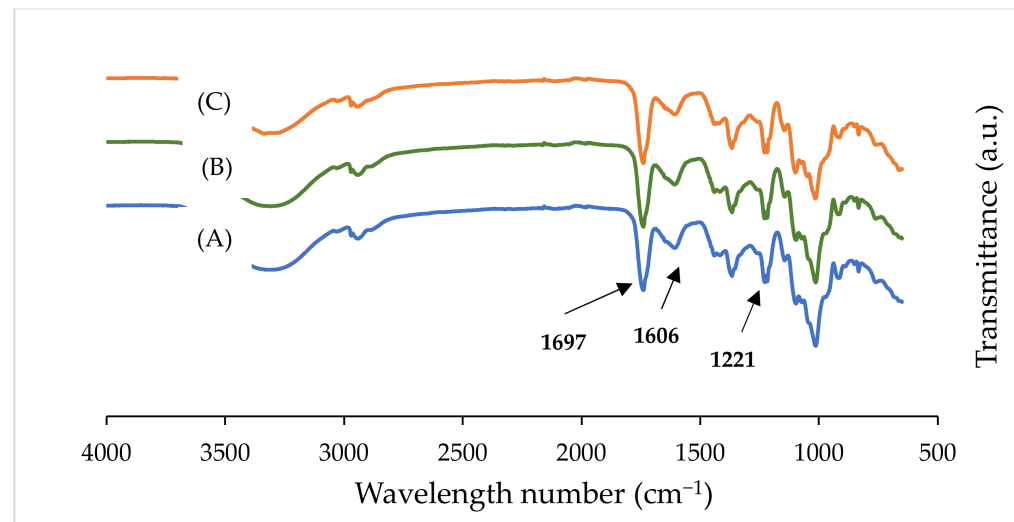

Figure 5. FTIR spectra of pectin films (**A**) incorporated with: (**B**) MMT and (**C**) CNC.

FTIR analysis was conducted to validate the effect of the deposition of pectin on chitosan. On analyzing bilayer films from both sides, no chemical modifications were observed (Figure 6). One of the sides of bilayer film depicted the spectrum of pure chitosan, while the pure pectin's spectrum was observed on the inverted side. The bonding of pure chitosan and pectin predominates over the interfacial interactions that exist between the two biopolymers. This can be attributed to the synthesis methodology used to cast these bilayer films. When pectin solution was poured onto the semi-dried chitosan film, there is a strong possibility that only interfacial/local interactions took place due to the reaction between protonated amino groups of chitosan and carboxylate side chains of pectin, which are responsible only for keeping these two polymers from binding together [43].

FTIR of bilayer films show that the dominated chitosan peaks at around 3256, 1550, 1406 and 1376 cm^{-1} decreased, confirming the incorporation of chitosan during the formation of pectin/chitosan films. Moreover, it is worth noting that the shifts on the peaks corresponding to OH (stretch) range from 3256 cm^{-1} to 3310 cm^{-1} and the amide groups peaks from 1617 cm^{-1} to 1605 cm^{-1}. These shifts are indicative of the ionic interaction that may have occurred between the anion carboxylate groups of pectin and NH$_3^+$ from chitosan [44]. Thus, this corroborates the SEM images (Figure 4) that depict the good interaction of the polysaccharides in this bilayer.
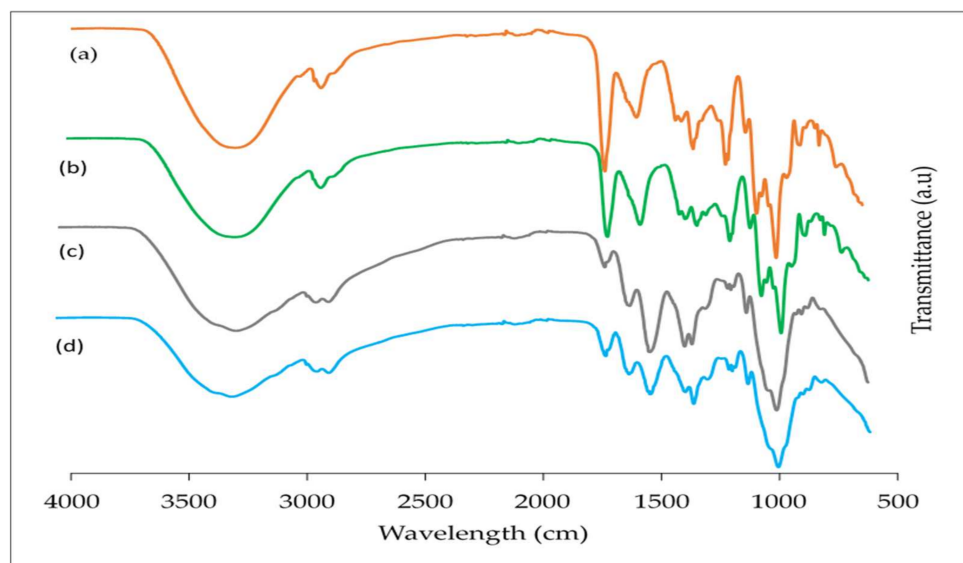
Figure 6. FTIR spectra of pure pectin (**a**), chitosan films (**c**) and bilayer films from both sides ((**b**) and (**d**)).

3.1.3. Optical Properties

Color and opacity are crucial parameters for the development of food packing films [45]. They are not only important from an aesthetics point of view, but also for the protection of food from UV and visible light. The presence of UV light can catalyze oxidation reactions, which can deteriorate food, reducing its shelf-life and nutritional value [24].

The values of chroma, hue angle and opacity are shown in Table 1. Overall, the color of the films was not changed due to the incorporation of the NPs, as both the chroma and hue angle were not affected ($p > 0.05$). The resultant bilayer film depicts higher chroma (more saturated color) when compared to individual neat films. This is because of the addition of chitosan on one side of the pectin film, which enhances the chroma. Moreover, the interfacial denser region might also be responsible for this higher chroma value reported for the bilayer.

Table 1. Optical properties of the films.

Film	Chroma	Hue Angle (°)	Opacity (mm^{-1})
P	11.3 ± 0.4 [A]	89.4 ± 0.2 [B]	1.51 ± 0.28 [AB]
P + 2.5%MMT	11.9 ± 1.2 [A]	89.5 ± 1.2 [B]	1.42 ± 0.28 [AB]
P + 2.5%CNC	10.8 ± 0.4 [A]	91.0 ± 0.2 [B]	2.40 ± 0.73 [A]
Bilayer	12.6 ± 0.2 [A]	93.6 ± 0.2 [A]	1.20 ± 0.14 [B]
Chitosan	9.1 ± 0.1	99.3 ± 0.1	0.70 ± 0.10

Superscript letters (A,B): different superscripts within the same column indicate significant differences among formulations ($p < 0.05$). P: Pectin, MMT: sodium montmorillonite, CNC: cellulose nanocrystals.

The hue angle range was around 90°, which confirms the yellowish color observed with the naked eye and previously reported in the literature for pectin powder and films [46]. In the case of the bilayer film, the incorporation of the chitosan layer to the composite resulted in a hue angle superior to pectin stand-alone films, which means that the resulting color of the bilayer film was between the color of the chitosan and pectin stand-alone films, as its hue angle was 93.6°. Similar behavior have been observed in bilayer films of Fucopol (a microbial polymer (fucose-rich exopolysaccharide) produced by *Enterobacter* A47) and chitosan, where the resulting color of the bilayer was between the initial color of the stand-alone films used to produce the bilayer [31].

The opacity of pectin films was not affected by the addition of either the NPs tested (CNC or MMT) nor the chitosan layer ($p > 0.05$). Despite the non-statistical difference

between the samples, films with CNC presented a 60% increase in opacity in comparison to pristine pectin films, which is, however, a trend already reported in the literature when nanoparticles are included in the polymeric matrices [22,47]. The increase in opacity of films is undesirable considering that films for food packaging should be transparent [46]; however, our results are in the same order of magnitude as some commonly used synthetic polymers such as low density polyethylene (3.05 A_{600}/mm) and oriented polypropylene (1.67 A_{600}/mm), which are considered to be transparent plastics [31,48]. In the case of MMT, once the montmorillonite layers have smaller thicknesses than the wavelength of visible light, they do not divert light and are transparent, and thus this does not reflect an increase in the bionanocomposites' opacity [38,49].

The increase in opacity with the addition of CNC agrees with the internal transmittance spectrum, where the presence of these nanoparticles reduced the transparency of the film in the visible region (data not shown). Neither fillers were able to reduce the transparency in the UV region, which would be an advantage against the deterioration of food products [38].

Bilayer films presented a resulting opacity which was equal to the average of the stand-alone films opacities, which corroborates with the other optical properties evaluated, and is in good agreement with results the literature [31,48].

3.1.4. Contact Angle

Contact angle (CA) measurements were conducted to determine the surface wettability of the synthesized films and are reported in Table 2. Despite small morphological changes (Figures 3 and 4), alterations in the CA were depicted. The CNC NPs increased the contact angle of the films by 3%, but with no statistical significance ($p > 0.05$), while montmorillonite caused a 15% increase in this property ($p < 0.05$). This is an indication that the NPs made the films less hydrophilic, which is coherent with the reduction in the WVP (Section 3.1.5). The literature relates the reduction of WVP in bionanocomposite films with the increase of the contact angle [50].

Table 2. Contact angle, swelling and humidity of the films.

Film	Contact Angle (°)	Humidity (%)	Swelling (%)
P	62.3 ± 0.7 [C]	13.5 ± 0.7 [A]	Dissolved
P + 2.5%MMT	76.7 ± 4.5 [B]	13.3 ± 0.6 [A]	Dissolved
P + 2.5%CNC	65.0 ± 2.8 [C]	12.2 ± 0.8 [A]	Dissolved
Bilayer	63.8 ± 0.5 [C]	13.3 ± 0.5 [A]	278 ± 80
Bilayer inverted	89.5 ± 0.7 [A]	NA	NA
Chitosan	93.1 ± 0.1	11.3 ± 0.4	170 ± 16

Superscript letters (A–C): different superscripts within the same column indicate significant differences among formulations ($p < 0.05$). P: Pectin, MMT: sodium montmorillonite, CNC: cellulose nanocrystals, NA: Not applied, bilayer- upper surface pectin, bilayer inverted- upper surface chitosan.

It was observed that chitosan has a higher contact angle when compared to pectin, which makes chitosan more hydrophobic when compared to pectin. A similar trend was observed by Farris et al. (2011) [51]. The hydrophilicity of pectin can be attributed to the presence of water-soluble carbohydrate groups in its backbone chain [22]. For the bilayer film, each side depicted a contact angle similar to their corresponding stand-alone biopolymer, pectin or chitosan.

3.1.5. Humidity, Solubility and Swelling Degree

The humidity of all films was the same ($p > 0.05$). Hence, the inclusion of the nanofillers or the bilayer with chitosan did not impact the capacity of the matrix to retain water molecules (Table 2). Despite being statistically insignificant, a slightly decrease of the water content of the films with the incorporation of either NPs could be observed, which is in good agreement with the results reported in the literature for pectin film reinforced with silver nanoparticles [52] or montmorillonite [22].

The water solubility and swelling index of the synthesized films were evaluated to study the material's degradability or resistance under an aqueous environment, and the capacity to absorb water, respectively [53]. It was found out that pectin was completely soluble in water (100%), even when the nanoparticles were incorporated (Table 2). This is due to the presence of water-soluble carbohydrates in its backbone chain [54]. Contrary to our results, other results from the literature indicate that pectin films may present a much lower solubility, e.g., 19% [55] or 52% [22], which could be explained by the different types of pectin used in different studies (and its degree of methylation). On the other hand, chitosan posed better resistance against water and approximately only $26.8 \pm 0.6\%$ of the polymer was water-soluble after 24 h of contact with water. This resistance can be attributed to the presence of intermolecular hydrogen bonding between the chains of chitosan. As expected, bilayer films showed an intermediate ($64.1 \pm 3.4\%$) response with regard to water solubility. Regarding the swelling index, once all pectin films had dissolved during the assay, Table 2 only presents those result for the bilayer and chitosan films. As expected, the bilayer films swelled more in water than the chitosan films, and this is due to the presence of the pectin that bonds well with water; however, this bilayer did not dissolve.

3.1.6. Water Vapor Permeability (WVP)

The barrier properties of food packaging films play a major role in defining the shelf-life of packed food/products. Reduced permeation of moisture and gaseous vapors across the packaging is always preferred [56].

Overall, due to their hydrophilic nature, polysaccharide polymers, such as chitosan and pectin, present high WVP [31]. The WVP of pristine pectin film was $2.15 \pm 0.28 \times 10^{-11}$ mol/m·s·Pa (Table 3), slightly smaller than the values of pristine chitosan film ($2.50 \pm 0.13 \times 10^{-11}$ mol/m·s·Pa) but within the same order of magnitude. These results are in good agreement with the reported WVP found in the literature for these polymers. Ferreira et al. (2016) [31] and Souza et al. (2021) [57] reported WVP values for chitosan films of 4.13×10^{-11} mol/m·s·Pa and 1.54×10^{-11} mol/m·s·Pa, respectively, and Yu et al. (2014) [58] reported 1.03×10^{-11} mol/m·s·Pa for pectin films, which are in the same range of the obtained results.

Table 3. Water vapor and oxygen permeability of the films and comparison with WVP data from literature.

Film	WVP		O_2 Permeability $(10^{-16}$ mol·m/m^2·s·Pa)	Reference
	Condition (Temperature °C/RH%)	$(10^{-11}$ mol/m·s·Pa)		
P	30 °C/RH 76.9–22.5%	2.15 ± 0.28 [B]	1.12 ± 0.02 [AB]	This work
P + 2.5% MMT	30 °C/RH 76.9–22.5%	1.45 ± 0.13 [C]	0.82 ± 0.02 [B]	This work
P + 2.5% CNC	30 °C/RH 76.9–22.5%	1.39 ± 0.11 [C]	0.46 ± 0.01 [B]	This work
Bilayer	30 °C/RH 76.9–22.5%	2.69 ± 0.13 [A]	1.68 ± 0.65 [A]	This work
Bilayer inverted	30 °C/RH 76.9–22.5%	NA	NA	This work
C	30 °C/RH 76.9–22.5%	2.50 ± 0.13	0.28 ± 0.06	This work
P	24 °C/RH 0%–100%	3.89	-	[22]
P + 2–8% MMT	24 °C/RH 0%–100%	2.33–3.35	-	[22]
P	25 °C/0%–52.8%	0.71	-	[59]
P + 2–7% CNC	25 °C/0%–52.8%	$\cong$0.51–0.58	-	[59]
P	25 °C/0%–100%	2.18 ± 0.40	-	[60]
P + CNP	25 °C/0%–100%	3.11 ± 0.23	-	[60]

Superscript letters (A–C): different superscripts within the same column indicate significant differences among formulations ($p < 0.05$). P: Pectin, MMT: sodium montmorillonite, CNC: cellulose nanocrystals, C: chitosan, CNP: chitosan nanoparticles, WVP: water vapor permeability, RH: relative humidity. NA: Not applied, bilayer- upper surface pectin, bilayer inverted- upper surface chitosan.

The average values for the WVP of the films with nano reinforcement were significantly reduced ($p < 0.05$). The incorporation of MMT and CNC decreased the WVP of the films by approximately 33% and 35%, respectively (Table 3). However, no significant difference was observed between the nanofillers tested ($p > 0.05$), indicating that both nanoparticles

are suitable to enhance the polymer barrier against water vapor. The decrease in the permeability shows that the nanoparticles imposed a longer and more tortuous permeation path for water vapor molecules when diffusing across the polymer matrix [58]. This is in agreement with the literature, where a decrease in permeability has been predicted and observed with the addition of a small amount (1%–8%) of nanofillers [26,61,62] (and some examples in Table 3). Bionanocomposites of pectin and silver nanoparticles (AgNPs) synthesized by a novel green method using an aqueous extract of *Caesalpinia mimosoides* Lamk presented a WVP 8.1% lower than pristine pectin films [52]. Therefore, these NPs presented a lower impact on the reduction of WVP than in our study. In the work of Oliveira et al. (2016) [22] (Table 3), pomegranate peel pectin films reinforced with MMT presented improved WVP with an increase in the percentage of NPs incorporated. Yet, comparing our results with this pomegranate peel pectin films [22], it is interesting to note that the incorporation of only 6–8 wt.% MMT, 2-fold the content in NPs used in our study, allowed for a reduction of the WVP similar (30%–40%) to the one obtained with the bionanocomposites of the current study.

According to the literature, bilayer films in general represent a more effective barrier against water vapor transfer than composite films [44,48]; however, contrary to what might be expected, the WVP of bilayer film was slightly higher than the WVP of the stand-alone films used to produce the bilayer and the bionanocomposites ($p < 0.05$), despite them being within the same order of magnitude. Blends and bilayers of edible films with increased WVP in comparison to the stand-alone films have been reported in the literature, specifically for blends of gelatin/chitosan [62]; brea gum/pectin [55]; caseinate/chitosan [63] and paper coated with a bilayer of caseinate/chitosan [44]. According to Pereda, Aranguren and Marcovich (2009) [63], the high humidity conditions used during the WVP test (100%–64.5% RH gradient) might affect the interactions between the biopolymers, causing changes in the microstructure conformation of the blends as a result of swelling, thus increasing the WVP, which might explain our results. Nonetheless, the experimental data obtained in the study lies in the same range of the calculated theoretical value of the permeability of multi-layer films, which can be estimated using the permeability and thickness of each individual layer [45]. Indeed, the calculated value of the WVP of the bilayer films gives 2.28×10^{-11} mol/m·s·Pa, which is between the values of pectin and chitosan and in agreement with the literature [42,48].

3.1.7. Oxygen Permeability (OP)

The values for the results of OP are reported in Table 3. Polysaccharide polymers, such as pectin and chitosan, are known for having good barrier properties against oxygen [21], even better than the traditional petroleum-based ones commonly used in the packaging industry. The nanoparticles incorporated into the films were able to reduce the bionanocomposites' OP in 26.8% and 58.9% for MMT and CNC, respectively, but with no statistical significance ($p > 0.05$). This result agrees with observations made in previous studies [61,64,65], and can be attributed to the presence of dispersed particles in the polymer that create a tortuous path delaying the transport of oxygen through the film [33]. Again, no statistical difference was observed between the nanoparticles studied ($p > 0.05$), but similar to the WVP results, pectin + CNC film presented smaller OP to pectin + MMT film.

A response similar to WVP was observed when the oxygen barrier properties of the bilayer film were studied. Bilayer films exhibited slightly higher oxygen permeation when compared to the neat pectin film, although this difference was not statistically significant. However, the results obtained are still better than fossil fuel-based low-density polyethylene (8.8×10^{-16} mol·m/m^2·Pa·s), which is widely used in food packaging [66].

3.1.8. Thickness and Mechanical Properties

The incorporation of the nanoparticles did not affect the thickness (Table 4) of the bionanocomposite films produced ($p > 0.05$), which corroborates with the SEM images (Figure 3). An increase in the bilayer thickness is also corroborated when compared with the

bionanocomposites. Although in the same order of magnitude, the values of the thickness observed with SEM are lower than the ones measured with the digital micrometer, most probably due to the dehydration caused by the high vacuum used in SEM operation conditions. Despite this non-statistical difference, bionanocomposites with CNC or MMT presented a slight reduction in the thickness, which can be correlated with a good interaction between the polymer and the NPs, which results in a more compact structure [33]. Similar behavior has been reported by Souza et al. (2018) [38] for bionanocomposites of chitosan reinforced with sodium montmorillonite, the thickness of which was 5% smaller than pristine chitosan film. Regarding the bilayer, the thickness slightly increased, as observed in the SEM images (Figure 4), but also with no statistical significance when compared to the pectin thickness value ($p > 0.05$). This trend was also reported for bilayers of chitosan and gelatin, with the bilayers presenting an increase between 8%–17% in comparison to stand-alone films, respectively, but also with no statistical significance ($p > 0.05$) [67].

Table 4. Mechanical properties of the films and comparison with data from literature.

Film	Thickness (µm)	Tensile Strength (MPa)	Elongation at Break (%)	Modulus of Elasticity (MPa)	Reference
P	83.7 ± 3.5 ^{AB}	22.3 ± 2.5 ^{AB}	4.3 ± 0.3 ^{AB}	1027 ± 127 ^{AB}	This work
P + 2.5%MMT	74.0 ± 7.9 ^{B}	24.2 ± 4.2 ^{AB}	3.7 ± 0.7 ^{AB}	1227 ± 215 ^{A}	This work
P + 2.5%CNC	67.3 ± 9.7 ^{B}	30.8 ± 4.0 ^{A}	3.5 ± 1.0 ^{B}	1407 ± 178 ^{A}	This work
Bilayer	93.0 ± 4.0 ^{A}	16.7 ± 2.7 ^{B}	5.4 ± 0.5 ^{A}	779 ± 131 ^{B}	This work
C	98.2 ± 3.6	8.5 ± 1.5	39.4 ± 2.3	155 ± 25	This work
P	-	2.42	6.55	189.53	[22]
P + 2–8%MMT	-	3.27–4.25	6.01–5.35	288.6–318.7	[22]
P	-	7.12	≅20	-	[59]
P + 2–7% CNC	-	≅8.00–13.15	≅25–40	-	[59]
P	-	25.9 ± 1.9	35.5 ± 1.7	-	[54]
Blend of P + C (50:50)	-	≅18	≅33	-	[54]
P	-	30.81 ± 1.50	1.79 ± 0.27	-	[60]
P + CNP	-	46.95 ± 0.36	2.22 ± 0.56	-	[60]

Superscript letters (A,B): different superscripts within the same column indicate significant differences among formulations ($p < 0.05$). P: Pectin, MMT: sodium montmorillonite, CNC: cellulose nanocrystals, C: chitosan, CNP: chitosan nanoparticles.

The changes in the mechanical properties of the films were not statistically different ($p > 0.05$). Nevertheless, an increase of 38.1% and 37% was observed in the average tensile strength and elasticity modus, respectively, of the films incorporated with CNC, as well as a decrease of 22.9% in the elongation at break (Table 4). This effect has been reported previously and was attributed to the formation of a continuous network of cellulosic nanoparticles linked through hydrogen bonding [59,68]. Other researchers found similar results when CNC was added to polysaccharides such as alginate [69] and chitosan [38].

The slight improvement of the mechanical properties of the films with the incorporation of sodium montmorillonite was not as evident as for CNC, as the average tensile strength and elasticity modulus only increased 8.5% and 19.5%, respectively, while the elongation at break reduced 14%. However, again no statistical difference was observed between the bionanocomposites. It has been established that the type of nanofiller also has an effect on the properties of films [70], and once this has been taken into account, the small differences observed in the mechanical behavior of the bionanocomposites might be related to the nature of the NPs, as MMT is inorganic with platelet like morphology (Figure 3b) and CNC is organic with fiber morphology (Figure 3a) and a different interaction with the polymer that may result from various structural and arrangement features [70]. As discussed in the XRD results for bionanocomposites with MMT, the achievement of the exfoliated configuration can explain this small change, which in fact represents an improvement in the mechanical properties [18].

The pectin and chitosan responded in opposite ways (Table 4). Pectin was found to be brittle in nature while the chitosan showed a ductile response (Figure 7).
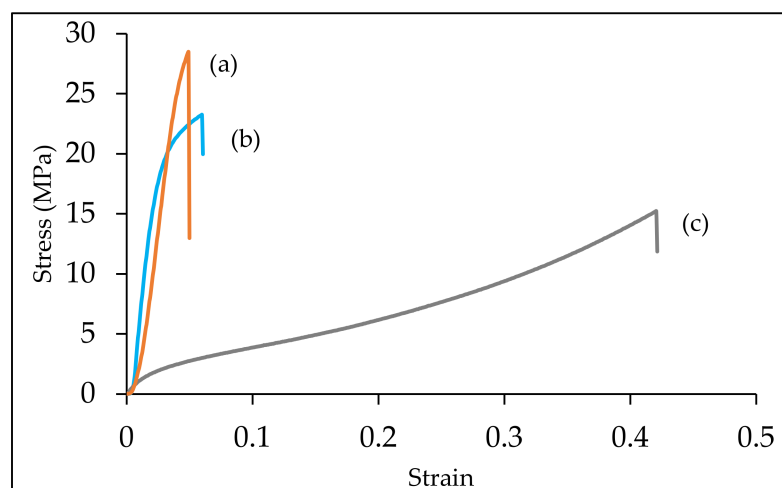
Figure 7. Stress–strain curves of pristine pectin (**a**), bilayer (**b**) and pristine chitosan films (**c**).

Deposition of pectin onto chitosan improved the tensile strength by 2-fold while the Young modulus was improved by 5-fold. In short, bilayer films presented the average values of the mechanical characteristics of both polymers. Similar improvements were also observed by Baron et al. in 50:50 chitosan and pectin blend films [54]. While the elongation at break (EAB) of bilayer film did not show any intermediate values, it was very close to the neat pectin films. It is possible that this is due to the surface irregularities which serve as stress concentration points and cause fractures at low strain.

It should be pointed out that these bilayer films behaved as a homogenous system on the application of stress. No phase/layer separation was observed even upon rupture, which corroborates with the SEM image in Figure 4.

3.1.9. Exposure to the Use of Nanoparticles in Food Packaging Materials

The aim is that this material is to be used by the food industry in direct contact with foodstuffs in the context of packaging them, and so it is mandatory to address their safety and assess whether the inclusion of the nanoparticles pose any risk to the consumers [71].

To evaluate the exposure of consumers to a nanomaterial from a food packaging, it is fundamental to determine if there is migration of this NP from the food contact material (FCM) into the food matrix, and if so, the extend of the actual migration [72]. Thus, in addition to the characterization of the pristine NPs used to produce the packaging, a further characterization is necessary of both NPs as present in the FCM (on the surface, in the matrix) and possibly when being released from the FCM (to confirm if they kept the nanoparticle form or are in solubilized (non-nanomaterial) form) [71,72]. And in the case of bio-based biodegradable polymers, their hydrophilicity and swelling properties may enhance the chances of the physical release of the NPs toward the food packaged. In which case, realistic migration/ release testing needs to be used under conditions that mimic their practical use without damaging the polymer performance properties [72]. However, this characterization is not easily done, as the NPs interact with the polymer and further with the food (in a potential scenario in which the NPs diffuse towards the food), which requires more robust techniques and steps, limiting this type of study and explaining the lack of information available [73,74].

The available information so far is mostly related to synthetic plastics, and according to the EFSA, it was concluded that no significant migration or transfer of the nanoparticles (carbon black, titanium nitrate, metal oxides and nanoclays) was expected under the defined conditions of use [72]. Moreover, after the nanoparticle migration, in several cases, they do not keep the nanoscale form, but are more likely to be solubilized, which reduces the risk associated with them [10,75].

For the NPs used in this study, this safety aspect was taken into consideration, as CNC and MMT are generally reported as safe [71]. Cellulose nanocrystals are reported in the literature to be non-cytotoxic, non-immunogenic, biodegradable, biocompatible and environmentally friendly [73]. Yet, size- and concentration may present a dependent effect. Cytotoxic effects may be induced by either the presence of a substantial proportion of particles with small sizes (below 50 nm) that might get taken up in high concentrations, or by larger size particles that can form gel in a suspension when incubated in high concentrations, which may block the passage of gases through the cell membranes [76]. Therefore, further investigations on CNC toxicity are required in order to have a better insight for their applications [77]. Regarding the MMT, a study was carried out with commercial nanoclays (including the unmodified sodium montmorillonite used in this work—Cloisite®Na⁺) and the authors demonstrated that Cloisite®Na⁺ was not cytotoxic and neither was it mutagenic within the range of the concentrations evaluated (from 0 to 62.5 μg/mL and 7.8 μg/mL to 125 μg/mL, respectively) [78].

3.1.10. Final Remarks

Overall, the strategy to improve the mechanical, optical and barrier properties of bio-based biodegradable polymers ranges from the inclusion of nanomaterial as reinforcement to the use of a mixture of polymers in composites as blends or as bilayers. In the specific case of pectin, it is possible to find good examples, as previously discussed in this paper. It is important to highlight that the results vary greatly, as the methodologies and materials used to prepare the films also vary. Currently, it is more common to find in the literature blends of polymers (such as pectin/PLA [79], *Aegle marmelos* pectin–chitosan [80], pectin/gluten [81], pectin/chitosan [82], to mention a few) over bilayers (e.g., brea gum/pectin [55]). From this point of view, this work evaluated both strategies by using two NPs as nanofillers and through the use of chitosan/pectin bilayer films. It is important to point out that all other parameters (such as the type and amount of plasticizer or the percentages of NPs incorporated) were maintained in order to make the comparison suitable. This systematic study has never been done, and based in our results, it is possible to suggest as future research the development of bilayers produced with stand-alone polymers reinforced with NPs to achieve a material with optimal properties combining both strategies.

4. Conclusions

Bionanocomposite films of pectin with cellulose nanocrystals and sodium montmorillonite were successfully produced. The incorporation of both nanoparticles significantly reduced the water vapor permeability of the films and increased their contact angle, showing that the fillers had the effect of reducing the hydrophilicity of pectin films. The particles did not affect the optical properties of the films, which is desirable for packaging purposes. However, the mechanical properties of the films were not statistically changed with the addition of the fillers, although the inclusion of CNC seemed to have caused an increase in the tensile strength and modulus of elasticity of the samples.

Regarding the safety of these materials, more studies are still necessary to evaluate whether the inclusion of NPs can pose a risk to consumers. However, taking into consideration the small amount of NPs incorporated, it is likely that the materials developed in this study do not pose a risk to the consumers.

Bilayer films of chitosan/pectin showed a transparent yellowish tint with a stiff homogenous structure. They presented a water vapor and oxygen barrier and mechanical properties similar to the pectin films; however, they did not dissolved in water, as in the case of the pectin nanocomposite films, which allows for their use in packing food with high moisture content. All the films presented higher oxygen barrier properties than LDPE, which is widely used in food packaging. So, these bio-based biodegradable films are good candidates to replace synthetic polymers from non-renewable sources for the packaging of low moisture content products. These films also have huge potential to be used as an inner layer for multilayer packaging for high moisture content products.

Based in on our results, it is possible to suggest as future research the development of bilayers produced with stand-alone polymers reinforced with NPs to achieve a material with optimal properties combining both strategies. By comparing the two strategies in the same study, it was possible to understand that a bilayer option helps to make pectin films more hydrophobic, which may play an important role in the application of pectin as a food packaging material, and that the mechanical and barrier properties of pectin-based films are improved when NPs are incorporated. In addition, it would be interesting to study, in a future work, if the active properties of the pectin films (e.g., antimicrobial and antioxidant) would be improved through the incorporation of nanofillers or the development of bilayers.

Author Contributions: Conceptualization, V.G.L.S., I.C. and A.L.F.; methodology, I.P.M., O.K., J.R.A.P. and C.R.; software, I.P.M. and O.K.; formal analysis, M.M.A., C.S., V.G.L.S., I.P.M., O.K., J.R.A.P. and C.R.; investigation, I.P.M., O.K., J.R.A.P. and C.R.; resources, V.G.L.S., I.C. and A.L.F.; writing—original draft preparation, I.P.M. and O.K.; writing—review and editing, V.G.L.S., I.C., M.M.A., C.S. and A.L.F.; supervision, V.G.L.S., I.C. and A.L.F.; funding acquisition, I.C. and A.L.F. All authors have read and agreed to the published version of the manuscript.

Institutional Review Board Statement: Not applicable.

Informed Consent Statement: Not applicable.

Data Availability Statement: Data is contained within the article.

Conflicts of Interest: The authors declare no conflict of interest.

References

1. FAO. *Mitigation of Food Waste: Societal Costs and Benefits*; FAO: Rome, Italy, 2014; ISBN 978-92-5-108511-0.
2. FAO. *Global Food Losses and Food Waste—Extent, Causes and Prevention*; FAO: Rome, Italy, 2011; ISBN 9789251072059.
3. Wikström, F.; Verghese, K.; Auras, R.; Olsson, A.; Williams, H.; Wever, R.; Grönman, K.; Kvalvåg Pettersen, M.; Møller, H.; Soukka, R. Packaging Strategies That Save Food: A Research Agenda for 2030. *J. Ind. Ecol.* **2019**, *23*, 532–540. [CrossRef]
4. Dilkes-Hoffman, L.S.; Lane, J.L.; Grant, T.; Pratt, S.; Lant, P.A.; Laycock, B. Environmental impact of biodegradable food packaging when considering food waste. *J. Clean. Prod.* **2018**, *180*, 325–334. [CrossRef]
5. Wikström, F.; Williams, H.; Verghese, K.; Clune, S. The influence of packaging attributes on consumer behaviour in food-packaging life cycle assessment studies—A neglected topic. *J. Clean. Prod.* **2014**, *73*, 100–108. [CrossRef]
6. Souza, V.G.L.; Pires, J.R.A.; Rodrigues, C.; Coelhoso, I.M.; Fernando, A.L. Chitosan Composites in Packaging Industry—Current Trends and Future Challenges. *Polymers* **2020**, *12*, 417. [CrossRef] [PubMed]
7. Andrade, M.A.; Barbosa, C.H.; Souza, V.G.L.; Coelhoso, I.M.; Reboleira, J.; Bernardino, S.; Ganhão, R.; Mendes, S.; Fernando, A.L.; Vilarinho, F.; et al. Novel Active Food Packaging Films Based on Whey Protein Incorporated with Seaweed Extract: Development, Characterization, and Application in Fresh Poultry Meat. *Coatings* **2021**, *11*, 229. [CrossRef]
8. Kaur, G.; Uisan, K.; Ong, K.L.; Ki Lin, C.S. Recent Trends in Green and Sustainable Chemistry & Waste Valorisation: Rethinking Plastics in a circular economy. *Curr. Opin. Green Sustain. Chem.* **2018**, *9*, 30–39. [CrossRef]
9. Pobiega, K.; Igielska, M.; Włodarczyk, P.; Gniewosz, M. The use of pullulan coatings with propolis extract to extend the shelf life of blueberry (Vaccinium corymbosum) fruit. *Int. J. Food Sci. Technol.* **2021**, *56*, 1013–1020. [CrossRef]
10. Souza, V.G.L; Rodrigues, C.; Valente, S.; Pimenta, C.; Pires, J.R.A.; Alves, M.M.; Santos, C.F.; Coelhoso, I.M.; Fernando, A.L.L. Eco-Friendly ZnO/Chitosan Bionanocomposites Films for Packaging of Fresh Poultry Meat. *Coatings* **2020**, *10*, 110. [CrossRef]
11. Souza, V.G.L.; Rodrigues, C.; Ferreira, L.; Pires, J.R.A.; Duarte, M.P.; Coelhoso, I.; Fernando, A.L. In vitro bioactivity of novel chitosan bionanocomposites incorporated with different essential oils. *Ind. Crops Prod.* **2019**, *140*, 111563. [CrossRef]

12. Tkaczewska, J. Peptides and protein hydrolysates as food preservatives and bioactive components of edible films and coatings—A review. *Trends Food Sci. Technol.* **2020**, *106*, 298–311. [CrossRef]

13. Hoagland, P.D.; Parris, N. Chitosan/pectin laminated films. *J. Agric. Food Chem.* **1996**, *44*, 1915–1919. [CrossRef]

14. Mesbahi, G.; Jamalian, J.; Farahnaky, A. A comparative study on functional properties of beet and citrus pectins in food systems. *Food Hydrocoll.* **2005**, *19*, 731–738. [CrossRef]

15. Tripathi, S.; Mehrotra, G.K.; Dutta, P.K. Preparation and physicochemical evaluation of chitosan/poly(vinyl alcohol)/pectin ternary film for food-packaging applications. *Carbohydr. Polym.* **2010**, *79*, 711–716. [CrossRef]

16. Freitas, C.M.P.; Coimbra, J.S.R.; Souza, V.G.L.; Sousa, R.C.S. Structure and Applications of Pectin in Food, Biomedical, and Pharmaceutical Industry: A Review. *Coatings* **2021**, *11*, 922. [CrossRef]

17. Laurent, M.A.; Boulenguer, P. Stabilization mechanism of acid dairy drinks (ADD) induced by pectin. *Food Hydrocoll.* **2003**, *17*, 445–454. [CrossRef]

18. Rhim, J.-W.; Ng, P.K.W. Natural biopolymer-based nanocomposite films for packaging applications. *Crit. Rev. Food Sci. Nutr.* **2007**, *47*, 411–433. [CrossRef] [PubMed]

19. Otoni, C.G.; Moura, M.R.D.; Aouada, F.A.; Camilloto, G.P.; Cruz, R.S.; Lorevice, M.V.; Soares, N.D.F.F.; Mattoso, L.H.C. Antimicrobial and physical-mechanical properties of pectin/papaya puree/cinnamaldehyde nanoemulsion edible composite films. *Food Hydrocoll.* **2014**, *41*, 188–194. [CrossRef]

20. Ferreira, A.R.V.; Alves, V.D.; Coelhoso, I.M. Polysaccharide-based membranes in food packaging applications. *Membranes* **2016**, *6*, 22. [CrossRef]

21. Alves, V.D.; Costa, N.; Coelhoso, I.M. Barrier properties of biodegradable composite films based on kappa-carrageenan/pectin blends and mica flakes. *Carbohydr. Polym.* **2010**, *79*, 269–276. [CrossRef]

22. Oliveira, T.Í.S.; Zea-Redondo, L.; Moates, G.K.; Wellner, N.; Cross, K.; Waldron, K.W.; Azeredo, H.M.C. Pomegranate peel pectin films as affected by montmorillonite. *Food Chem.* **2016**, *198*, 107–112. [CrossRef] [PubMed]

23. Pires, J.; Paula, C.D.D.; Souza, V.G.L.; Fernando, A.L.; Coelhoso, I. Understanding the Barrier and Mechanical Behavior of Different Nanofillers in Chitosan Films for Food Packaging. *Polymers* **2021**, *13*, 721. [CrossRef]

24. Souza, V.G.L.; Pires, J.R.A.; Rodrigues, C.; Rodrigues, P.F.; Lopes, A.; Silva, R.J.; Caldeira, J.; Duarte, M.P.; Fernandes, F.B.; Coelhoso, I.M.; et al. Physical and Morphological Characterization of Chitosan/Montmorillonite Films Incorporated with Ginger Essential Oil. *Coatings* **2019**, *9*, 700. [CrossRef]

25. Pires, J.R.A.; Souza, V.G.L.; Fernando, A.L. Valorization of energy crops as a source for nanocellulose production—Current knowledge and future prospects. *Ind. Crops Prod.* **2019**, *140*, 111642. [CrossRef]

26. Azeredo, H.M.C.; Rosa, M.F.; Mattoso, L.H.C. Nanocellulose in bio-based food packaging applications. *Ind. Crops Prod.* **2017**, *97*, 664–671. [CrossRef]

27. Younis, H.G.R.; Abdellatif, H.R.S.; Ye, F.; Zhao, G. Tuning the physicochemical properties of apple pectin films by incorporating chitosan/pectin fiber. *Int. J. Biol. Macromol.* **2020**, *159*, 213–221. [CrossRef]

28. Nowzari, F.; Shábanpour, B.; Ojagh, S.M. Comparison of chitosan-gelatin composite and bilayer coating and film effect on the quality of refrigerated rainbow trout. *Food Chem.* **2013**, *141*, 1667–1672. [CrossRef] [PubMed]

29. Luo, Y.; Wang, Q. Recent development of chitosan-based polyelectrolyte complexes with natural polysaccharides for drug delivery. *Int. J. Biol. Macromol.* **2014**, *64*, 353–367. [CrossRef] [PubMed]

30. Yin, Y.; Li, Z.; Sun, Y.; Yao, K. A preliminary study on chitosan/gelatin polyelectrolyte complex formation. *J. Mater. Sci.* **2005**, *40*, 4649–4652. [CrossRef]

31. Ferreira, A.R.V.; Torres, C.A.V.; Freitas, F.; Sevrin, C.; Grandfils, C.; Reis, M.A.M.; Alves, V.D.; Coelhoso, I.M. Development and characterization of bilayer films of FucoPol and chitosan. *Carbohydr. Polym.* **2016**, *147*, 8–15. [CrossRef] [PubMed]

32. ASTM. *Standard Test Method for Tensile Properties of Thin Plastic Sheeting—D882-12*; ASTM: West Conshohocken, PA, USA, 2012; Volume D882.

33. Souza, V.G.L.; Pires, J.R.A.; Vieira, É.T.; Coelhoso, I.M.; Duarte, M.P.; Fernando, A.L. Activity of chitosan-montmorillonite bionanocomposites incorporated with rosemary essential oil: From in vitro assays to application in fresh poultry meat. *Food Hydrocoll.* **2019**, *89*, 241–252. [CrossRef]

34. Zhuang, G.; Zhang, Z.; Peng, S.; Gao, J.; Pereira, F.A.R.; Jaber, M. The Interaction between Surfactants and Montmorillonite and its Influence on the Properties of Organo-Montmorillonite in Oil-Based Drilling FluIDS. *Clays Clay Miner.* **2019**, *67*, 190–208. [CrossRef]

35. Gong, J.; Li, J.; Xu, J.; Xiang, Z.; Mo, L. Research on cellulose nanocrystals produced from cellulose sources with various polymorphs. *RSC Adv.* **2017**, *7*, 33486–33493. [CrossRef]

36. Gaona-Sánchez, V.A.; Calderón-Domínguez, G.; Morales-Sánchez, E.; Chanona-Pérez, J.J.; Arzate-Vázquez, I.; Terrés-Rojas, E. Pectin-based films produced by electrospraying. *J. Appl. Polym. Sci.* **2016**, *133*, 43779. [CrossRef]

37. Silvestre, C.; Duraccio, D.; Cimmino, S. Food packaging based on polymer nanomaterials. *Prog. Polym. Sci.* **2011**, *36*, 1766–1782. [CrossRef]

38. Souza, V.G.L.; Pires, J.R.A.; Rodrigues, P.F.; Lopes, A.A.S.; Fernandes, F.M.B.; Duarte, M.P.; Coelhoso, I.M.; Fernando, A.L. Bionanocomposites of chitosan/montmorillonite incorporated with Rosmarinus officinalis essential oil: Development and physical characterization. *Food Packag. Shelf Life* **2018**, *16*, 148–156. [CrossRef]

39. Lavorgna, M.; Piscitelli, F.; Mangiacapra, P.; Buonocore, G.G. Study of the combined effect of both clay and glycerol plasticizer on the properties of chitosan films. *Carbohydr. Polym.* **2010**, *82*, 291–298. [CrossRef]

40. Billah, R.E.K.; Abdellaoui, Y.; Anfar, Z.; Giácoman-Vallejos, G.; Agunaou, M.; Soufiane, A. Synthesis and Characterization of Chitosan/Fluorapatite Composites for the Removal of Cr (VI) from Aqueous Solutions and Optimized Parameters. *Water Air Soil Pollut.* **2020**, *231*, 163. [CrossRef]

41. Woranuch, S.; Yoksan, R. Eugenol-loaded chitosan nanoparticles: I. Thermal stability improvement of eugenol through encapsulation. *Carbohydr. Polym.* **2013**, *96*, 578–585. [CrossRef] [PubMed]

42. Hileuskaya, A.; Ihnatsyeu-Kachan, A.; Kraskouski, A.; Salamianski, A.; Nikalaichuk, V.; Hileuskaya, K.; Kim, S. LbL films and microcapsules based on protamine and pectin-Ag nanocomposite. *Mater. Today Proc.* **2021**. [CrossRef]

43. Parris, N.; Coffin, D.R. Composition Factors Affecting the Water Vapor Permeability and Tensile Properties of Hydrophilic Zein Films. *J. Agric. Food Chem.* **1997**, *45*, 1596–1599. [CrossRef]

44. Khwaldia, K.; Basta, A.H.; Aloui, H.; El-Saied, H. Chitosan-caseinate bilayer coatings for paper packaging materials. *Carbohydr. Polym.* **2014**, *99*, 508–516. [CrossRef] [PubMed]

45. Peng, Y.; Li, Y. Combined effects of two kinds of essential oils on physical, mechanical and structural properties of chitosan films. *Food Hydrocoll.* **2014**, *36*, 287–293. [CrossRef]

46. Gouveia, T.I.A.; Biernacki, K.; Castro, M.C.R.; Gonçalves, M.P.; Souza, H.K.S. A new approach to develop biodegradable films based on thermoplastic pectin. *Food Hydrocoll.* **2019**, *97*, 105175. [CrossRef]

47. Vejdan, A.; Ojagh, S.M.; Adeli, A.; Abdollahi, M. Effect of TiO$_2$ nanoparticles on the physico-mechanical and ultraviolet light barrier properties of fish gelatin/agar bilayer film. *LWT Food Sci. Technol.* **2016**, *71*, 88–95. [CrossRef]

48. Rivero, S.; García, M.A.; Pinotti, A. Composite and bi-layer films based on gelatin and chitosan. *J. Food Eng.* **2009**, *90*, 531–539. [CrossRef]

49. Dias, M.V.; Machado Azevedo, V.; Borges, S.V.; Soares, N.D.F.F.; de Barros Fernandes, R.V.; Marques, J.J.; Medeiros, É.A.A. Development of chitosan/montmorillonite nanocomposites with encapsulated α-tocopherol. *Food Chem.* **2014**, *165*, 323–329. [CrossRef]

50. Da Silva, I.S.V.; Neto, W.P.F.; Silvério, H.A.; Pasquini, D.; Zeni Andrade, M.; Otaguro, H. Mechanical, thermal and barrier properties of pectin/cellulose nanocrystal nanocomposite films and their effect on the storability of strawberries (Fragaria ananassa). *Polym. Adv. Technol.* **2017**, *28*, 1005–1012. [CrossRef]

51. Farris, S.; Introzzi, L.; Biagioni, P.; Holz, T.; Schiraldi, A.; Piergiovanni, L. Wetting of biopolymer coatings: Contact angle kinetics and image analysis investigation. *Langmuir* **2011**, *27*, 7563–7574. [CrossRef] [PubMed]

52. Shankar, S.; Tanomrod, N.; Rawdkuen, S.; Rhim, J.W. Preparation of pectin/silver nanoparticles composite films with UV-light barrier and properties. *Int. J. Biol. Macromol.* **2016**, *92*, 842–849. [CrossRef] [PubMed]

53. Nunes, C.; Maricato, É.; Cunha, Â.; Nunes, A.; da Silva, J.A.L.; Coimbra, M.A. Chitosan-caffeic acid-genipin films presenting enhanced antioxidant activity and stability in acidic media. *Carbohydr. Polym.* **2013**, *91*, 236–243. [CrossRef] [PubMed]

54. Baron, R.D.; Pérez, L.L.; Salcedo, J.M.; Córdoba, L.P.; Sobral, P.J.D.A. Production and characterization of films based on blends of chitosan from blue crab (Callinectes sapidus) waste and pectin from Orange (Citrus sinensis Osbeck) peel. *Int. J. Biol. Macromol.* **2017**, *98*, 676–683. [CrossRef] [PubMed]

55. Slavutsky, A.M.; Gamboni, J.E.; Bertuzzi, M.A. Formulation and characterization of bilayer films based on Brea gum and Pectin. *Brazilian J. Food Technol.* **2018**, *21*, e2017213. [CrossRef]

56. Vilarinho, F.; Andrade, M.; Buonocore, G.G.; Stanzione, M.; Vaz, M.F.; Sanches Silva, A. Monitoring lipid oxidation in a processed meat product packaged with nanocomposite poly(lactic acid) film. *Eur. Polym. J.* **2018**, *98*, 362–367. [CrossRef]

57. Souza, V.G.L.; Alves, M.M.; Santos, C.F.; Ribeiro, I.A.C.; Rodrigues, C.; Coelhoso, I.; Fernando, A.L. Biodegradable chitosan films with ZnO nanoparticles synthesized using food industry by-products—Production and characterization. *Coatings* **2021**, *11*, 646. [CrossRef]

58. Yu, W.-X.; Wang, Z.-W.; Hu, C.-Y.; Wang, L. Properties of low methoxyl pectin-carboxymethyl cellulose based on montmorillonite nanocomposite films. *Int. J. Food Sci. Technol.* **2014**, *49*, 2592–2601. [CrossRef]

59. Chaichi, M.; Hashemi, M.; Badii, F.; Mohammadi, A. Preparation and characterization of a novel bionanocomposite edible film based on pectin and crystalline nanocellulose. *Carbohydr. Polym.* **2017**, *157*, 167–175. [CrossRef] [PubMed]

60. Lorevice, M.V.; Otoni, C.G.; de Moura, M.R.; Mattoso, L.H.C. Chitosan nanoparticles on the improvement of thermal, barrier, and mechanical properties of high- and low-methyl pectin films. *Food Hydrocoll.* **2016**, *52*, 732–740. [CrossRef]

61. Paul, D.R.; Robeson, L.M. Polymer nanotechnology: Nanocomposites. *Polymer* **2008**, *49*, 3187–3204. [CrossRef]

62. Fakhreddin Hosseini, S.; Rezaei, M.; Zandi, M.; Ghavi, F.F. Preparation and functional properties of fish gelatin-chitosan blend edible films. *Food Chem.* **2013**, *136*, 1490–1495. [CrossRef]

63. Pereda, M.; Aranguren, M.I.; Marcovich, N.E. Water vapor absorption and permeability of films based on chitosan and sodium caseinate. *J. Appl. Polym. Sci.* **2009**, *111*, 2777–2784. [CrossRef]

64. Giannakas, A.; Patsaoura, A.; Barkoula, N.M.; Ladavos, A. A novel solution blending method for using olive oil and corn oil as plasticizers in chitosan based organoclay nanocomposites. *Carbohydr. Polym.* **2017**, *157*, 550–557. [CrossRef] [PubMed]

65. Nouri, A.; Yaraki, M.T.; Ghorbanpour, M.; Agarwal, S.; Gupta, V.K. Enhanced Antibacterial effect of chitosan film using Montmorillonite/CuO nanocomposite. *Int. J. Biol. Macromol.* **2017**, *109*, 1219–1231. [CrossRef]

66. Ullsten, N.; Hedenqvist, M. A new test method based on head space analysis to determine permeability to oxygen and carbon dioxide of flexible packaging. *Polym. Test.* **2003**, *22*, 291–295. [CrossRef]
67. Pereda, M.; Ponce, A.G.; Marcovich, N.E.; Ruseckaite, R.A.; Martucci, J.F. Chitosan-gelatin composites and bi-layer films with potential antimicrobial activity. *Food Hydrocoll.* **2011**, *25*, 1372–1381. [CrossRef]
68. Habibi, Y.; Lucia, L.A.; Rojas, O.J. Cellulose nanocrystals: Chemistry, self-assembly, and applications. *Chem. Rev.* **2010**, *110*, 3479–3500. [CrossRef]
69. Abdollahi, M.; Alboofetileh, M.; Behrooz, R.; Rezaei, M.; Miraki, R. Reducing water sensitivity of alginate bio-nanocomposite film using cellulose nanoparticles. *Int. J. Biol. Macromol.* **2013**, *54*, 166–173. [CrossRef]
70. Jamróz, E.; Kulawik, P.; Kopel, P. The effect of nanofillers on the functional properties of biopolymer-based films: A review. *Polymers* **2019**, *11*, 675. [CrossRef]
71. Souza, V.G.L.; Ribeiro-Santos, R.; Rodrigues, P.F.; Otoni, C.G.; Duarte, M.P.; Coelhoso, I.M.; Fernando, A.L. Nanomaterial migration from composites into food matrices. In *Composite Materials for Food Packaging*; Cirillo, G., Kozlowski, M.A., Spizzirri, U.G., Eds.; Scrivener Publishing LLC: Beverly, MA, USA, 2018; pp. 401–435. ISBN 9781119160205.
72. More, S.; Bampidis, V.; Benford, D.; Bragard, C.; Halldorsson, T.; Hernández-Jerez, A.; Hougaard Bennekou, S.; Koutsoumanis, K.; Lambré, C.; Machera, K.; et al. Guidance on risk assessment of nanomaterials to be applied in the food and feed chain: Human and animal health. *EFSA J.* **2021**, *19*, e06768. [CrossRef] [PubMed]
73. Galvis-Sánchez, A.C.; Castro, M.C.R.; Biernacki, K.; Gonçalves, M.P.; Souza, H.K.S. Natural deep eutectic solvents as green plasticizers for chitosan thermoplastic production with controlled/desired mechanical and barrier properties. *Food Hydrocoll.* **2018**, *82*, 478–489. [CrossRef]
74. Ribeiro, A.R.; Leite, P.E.; Falagan-Lotsch, P.; Benetti, F.; Micheletti, C.; Budtz, H.C.; Jacobsen, N.R.; Lisboa-Filho, P.N.; Rocha, L.A.; Kühnel, D.; et al. Challenges on the toxicological predictions of engineered nanoparticles. *NanoImpact* **2017**, *8*, 59–72. [CrossRef]
75. European Food Safety Authority (EFSA). Safety assessment of the substance zinc oxide, nanoparticles, for use in food contact materials. *EFSA J.* **2016**, *14*, 4408. [CrossRef]
76. Hanif, Z.; Ahmed, F.R.; Shin, S.W.; Kim, Y.K.; Um, S.H. Size- and dose-dependent toxicity of cellulose nanocrystals (CNC) on human fibroblasts and colon adenocarcinoma. *Colloids Surf. B Biointerfaces* **2014**, *119*, 162–165. [CrossRef] [PubMed]
77. Trache, D.Y.; Tarchoun, A.F.; Derradji, M.; Hamidon, T.S.; Masruchin, N.; Brosse, N.; Hussin, M.H. Nanocellulose: From Fundamentals to Advanced Applications. *Front. Chem.* **2020**, *8*, 392. [CrossRef] [PubMed]
78. Maisanaba, S.; Prieto, A.I.; Pichardo, S.; Jordá-Beneyto, M.; Aucejo, S.; Jos, Á. Cytotoxicity and mutagenicity assessment of organomodified clays potentially used in food packaging. *Toxicol. In Vitro* **2015**, *29*, 1222–1230. [CrossRef] [PubMed]
79. Jin, T.; Liu, L.; Zhang, H.; Hicks, K. Antimicrobial activity of nisin incorporated in pectin and polylactic acid composite films against Listeria monocytogenes. *Int. J. Food Sci. Technol.* **2009**, *44*, 322–329. [CrossRef]
80. Jindal, M.; Kumar, V.; Rana, V.; Tiwary, A.K. An insight into the properties of Aegle marmelos pectin-chitosan cross-linked films. *Int. J. Biol. Macromol.* **2013**, *52*, 77–84. [CrossRef]
81. Sartori, T.; Feltre, G.; do Amaral Sobral, P.J.; Lopes da Cunha, R.; Menegalli, F.C. Properties of films produced from blends of pectin and gluten. *Food Packag. Shelf Life* **2018**, *18*, 221–229. [CrossRef]
82. Chetouani, A.; Follain, N.; Marais, S.; Rihouey, C.; Elkolli, M.; Bounekhel, M.; Benachour, D.; Le Cerf, D. Physicochemical properties and biological activities of novel blend films using oxidized pectin/chitosan. *Int. J. Biol. Macromol.* **2017**, *97*, 348–356. [CrossRef]